Regulation of breast tumorigenesis through acid sensors

Subash C. Gupta[1,2], **Ramesh Singh**[1,2], **Mathew Asters**[1], **Jianghua Liu**[1], **Xu Zhang**[3], **Mallikarjuna R. Pabbidi**[4], **Kounosuke Watabe**[5], and **Yin-Yuan Mo**[1,4]

[1]Cancer Institute, University of Mississippi Medical Center, Jackson, MS

[2]Department of Biochemistry, University of Mississippi Medical Center, Jackson, MS

[3]Center of Biostatistics and Bioinformatics, University of Mississippi Medical Center, Jackson, MS

[4]Department of Pharmacology and Toxicology, University of Mississippi Medical Center, Jackson, MS

[5]Department of Cancer Biology, Wake Forest University School of Medicine, Winston Salem, NC

Abstract

The low extracellular pH in the microenvironment has been shown to promote tumor growth and metastasis, however, the underlying mechanism is poorly understood. Particularly, little is known how the tumor cell senses the acidic signal to activate the acidosis-mediated signaling. In this study, we show that breast cancer cells express acid-sensing ion channel 1 (ASIC1), a proton-gated cation channel primarily expressed in the nervous system. RNA interference, knockout and rescue experiments demonstrate a critical role for ASIC1 in acidosis-induced reactive oxidative species and NF-κB activation, two key events for tumorigenesis. Mechanistically, ASIC1 is required for acidosis-mediated signaling through calcium influx. We show that as a cytoplasmic membrane protein, ASIC1 is also associated with mitochondria, suggesting that ASIC1 may regulate mitochondrial calcium influx. Importantly, interrogation of the Cancer Genome Atlas breast invasive carcinoma dataset indicates that alterations of ASIC1 alone or combined with other 4 ASIC genes are significantly correlated with poor patient survival. Furthermore, ASIC1 inhibitors cause a significant reduction of tumor growth and tumor load. Together, these results suggest that ASIC1 contributes to breast cancer pathogenesis in response to acidic tumor microenvironments, and ASIC1 may serve as a prognostic marker and a therapeutic target for breast cancer.

For correspondence: ymo@umc.edu; Phone: +1-601-815-6849; Fax: +1-601-815-6806.

CONFLICT OF INTEREST

The authors declare no conflict of interest.

INTRODUCTION

Breast cancer is a complex disease where close interaction of cancer cells with blood vessels, stromal cells and immune cells in the microenvironment regulates tumor growth and development. Because of disorganized tumor vasculature, heterogeneous blood flow, and increased glycolysis in tumor cells (Warburg effect), the tumor microenvironment is normally acidic (1). This acidic microenvironment (low extracellular pH, i.e., pHe-acidosis) affects tumor progression, invasion, metastasis and responses of tumors to chemotherapy and radiation (1). Previous studies from our laboratory and others have shown that acidic microenvironment contributes to breast tumor invasion and metastasis (2-5), which can be through activation of AKT and NF-κB, and generation of reactive oxygen species (ROS) (5-7). However, the upstream molecular drivers and underlying mechanism by which they impact invasiveness of cancer cells are poorly understood.

There are two major types of acid sensors in the cells, acid-sensing ion channels (ASICs) and proton-sensing G-protein coupled receptors (GPCRs) (8). ASICs belong to the subfamily of degenerin/epithelial Na^+ channels (Deg/ENaC) and are widely expressed throughout the central and peripheral nervous system (9), except for ASIC5 that is primarily expressed in the small intestine (10). The function of ASIC5 is not known. There are eight subunits of ASICs encoded by five different genes: ASIC1a, ASIC1b1, ASIC1b2, ASIC2a, ASIC2b, ASIC3, ASIC4 and ASIC5 (10-12). ASIC1 and ASIC2 have been shown to be upregulated in glioma, which is not surprising because they are derived from the same neuronal stem cells, as neuronal cells do. Furthermore, overexpression of ASICs is able to impact the growth and migration of glioblastoma cells (13, 14). For example, glioma cation current is mediated by mixed ASIC1 and ASIC2; inhibition of this conductance decreases glioma growth and cell migration (13). However, little is known whether ASICs are functionally expressed in epithelial cells or epithelia derived carcinoma such as mammary carcinoma and, if so, whether ASICs contribute to breast cancer pathogenesis.

Hence, the goal of the present study was to define the role of ASIC1 in breast tumorigenesis in the acidic microenvironment. Our results indicate that ASIC1 is a key player in acidosis-induced tumor growth and invasiveness. Clinically, alterations of ASIC1 are associated with poor survival in breast cancer.

RESULTS

Acidosis-induced ROS production is mediated through ASIC1 in breast cancer cells

Our recent study indicates that acidosis can enhance the invasion activity of breast cancer cells in a ROS-AKT-NF-κB dependent manner (5). However, it is not clear how the acidosis signal is transmitted into the tumor cell to activate the above pathway. In search of factors upstream to ROS-AKT-NF-κB signaling, we identified ASIC1 as a potential factor involved in acidosis-induced signaling because ASIC1 was expressed in a subset of breast cancer specimens and breast cancer cell lines although it is known to be primarily expressed in neuronal cells (15). For example, western blot analyses detected a high level of ASIC1 in MCF-7 and LM-4142 cells (Fig *1A*). Of interest, MMTV-Wnt1 cells which were derived from tumors of the MMTV-Wnt1 transgenic mouse also express a high level of ASIC1,

suggesting that ASIC1 is upregulated during tumorigenesis. In addition, we detected a high level of ASIC2a in LM-4142 cells.

Since ASIC1 functions as a key component of acid-activated currents (16) and it is much more sensitive to extracellular pH changes than ASIC2a (17), we decided to further characterize ASIC1. Acidosis can induce generation of ROS and ROS scavengers can suppress acidosis-induced invasion activity of breast cancer cells (5). Thus, we manipulated the ASIC1 activity or ASIC1 expression level to determine whether ASIC1 is required for acidosis-mediated ROS production. Cells (MCF-7, MDA-MB-231, LM-4142) were subject to acidosis (pH 6.6) for 1 h. We detected a significant ROS production in all of these 3 cell lines (Fig*1B*). Amiloride, a known pharmacological inhibitor for ASICs (18), significantly suppressed the acidosis-induced ROS production in MCF-7 cells (from 8.7 folds to 1.6 folds) (Fig*1C*) and in MDA-MB-231 cells (from 13.1 folds to 2.8 folds) (Fig *S1A*). Furthermore, psalmotoxin (PcTx1), a specific peptide inhibitor of ASIC1 (19), also significantly reduced the acidosis-induced ROS production (Fig*1D*, Fig *S1B*). Finally, ASIC1 siRNAs (Fig *S1C*) were also able to suppress the acidosis-induced ROS generation (Fig *1E*). Acidosis had no effect on ASIC1 expression (Fig *S1D*). Since NF-κB is a key factor in response to acidosis and responsible for the acidosis-induced invasion, we also determined the effect of ASIC1 inhibition or knockdown on activation of NF-κB. As shown in Fig. *S2A*, ASIC1 inhibitors (amiloride and PcTx-1) suppressed NF-κB activation. Similarly, ASIC1 siRNAs were also able to suppress acidosis-induced NF-κB activation (Fig. *S2B*).

To further determine the role of ASIC1 in acidosis-induced signaling in breast cancer, we knocked out ASIC1 in LM-4142 cells using CRISPR/Cas9 system (20) with a dual gRNA (Fig *S3*), an approach recently developed in our laboratory (21). As shown in Fig. *2A*, 2 out of 8 clones were complete knockouts, as determined by genomic PCR and western blot. In addition, we also identified a few other partial knockout (KO) clones. Flow cytometry analysis using Deep Red Reagent (DRR), a ROS labeling dye indicated that relative ROS production was a 2.5-fold in control cells whereas this number reduced to 1.6 in KO#1 cells (Fig*2B*, *left*). A similar result was also detected in KO#3 cells (Fig *2B*, *right*). Of great interest, the level of ROS generation induced by H_2O_2 was not significantly different between control and KO cells (Fig*2C*), suggesting that the ASIC1-mediated effect is specific to acidosis. To further define the role of ASIC1, we performed a rescue experiment, i.e., re-expression of Myc-tagged ASIC1 in ASIC1 KO cells (Fig *2D*). The re-expression of ASIC1 resulted in a 2-fold induction in ROS generation under acidic conditions, whereas there was no change in ROS generation in vector control cells (Fig *2E*). These results suggest that ASIC1 regulates ROS production in response to acidosis.

ASIC1 is required for acidosis-induced cell invasion, and tumor growth and lung metastasis

Since we previously showed that acidosis induces invasion activity of breast cancer cells (5), we asked whether ASIC1 is required for cell invasion. Matrigel invasion chamber assays indicated that invasion activity of control cells under acidic conditions was a 3.2-fold higher than that cultured at pH 7.4 (Fig *3A*). However, the invasion activity of ASIC1 KO cells

under acidic conditions was only a 1.7-fold higher than that cultured at pH 7.4. Rescue experiments revealed that re-expression of ASIC1 in KO cells caused a 2.8-fold increase in invasion activity as compared to a 1.9 fold increase in vector control cells (Fig*3B*). In addition, RNAi experiments also indicated that knockdown of ASIC1 caused a decrease in acidosis-induced invasion activity as compared to control siRNA (Fig *3C*), supporting a role for ASIC1 in the acidosis-induced invasion.

We then determined whether ASIC1 gene silencing can affect primary tumor growth in a xenograft mouse model. We transfected LM-4142 cells with control siRNA and ASIC1 siRNA and, then injected them into the mammary fat pads of female nude mice. We found that ASIC1 siRNA suppressed tumor growth as compared to control siRNA (Fig*4A, left*). Furthermore, the ASIC1 siRNA also reduced tumor weight by 45% (Fig *4A, middle*). A difference in the tumor size was visually obvious between the two groups (Fig *4A, right*), suggesting the role of ASIC1 in breast cancer primary tumor growth.

To determine whether ASIC1 impacts breast cancer metastasis *in vivo*, we performed an experimental metastasis assay with LM-4142, a lung metastatic cell line (22). Vector control and ASIC1 KO cells were injected into the tail vein of immunodeficient female mice. A gross examination of lungs at necropsy 6 weeks after tumor cell injection indicated that control cells exhibited a significant metastatic activity (lung tumor nodules) compared with the KO cells (Fig *4B*). Rescue experiments indicated that the number of nodules for the ASIC1 re-expressing cells was significantly higher than that with those injected with vector (Fig *4C*). Together, these results suggest that ASIC1 plays a critical role in cell invasion, tumor growth and metastasis.

ASIC1 is functional in LM-4142 cells

To determine the underlying mechanism by which ASIC1 mediates the acidosis-induced ROS production and breast tumorigenesis, we examined the functionality of ASIC1. Whole-cell patch-clamp recording using acidic pH-buffered solution indicated that while gRNA control cells responded to acidic solutions, ASIC1 KO abolished this response (Fig *5A*).

Since acidosis can induce an increase in intracellular calcium ($[Ca^{2+}]_i$) through activation of ASIC channels in neurons (23) and moreover, there is an association between Ca^{2+} uptake and ROS production (24, 25), we explored the possibility of involvement of Ca^{2+} in acidosis-induced ROS production. We tested the effects of intracellular (BAPTA-AM) and extracellular (EGTA) Ca^{2+} chelators. An assay using DRR indicated that acidosis induced a 2.1-fold increase in ROS generation that was completely suppressed by BAPTA-AM (Fig *5B*). However, in the presence of EGTA, acidosis-induced ROS generation was reduced from a 2.1-fold to a 1.2-fold, suggesting that Ca^{2+} plays an important role in the acidosis-induced ROS production in LM-4142 cells.

Given that chelation of intracellular calcium suppressed acidosis-induced ROS production, we asked whether acidosis can induce intracellular calcium level. LM-4142 cells were cultured under normal or low pH medium and loaded with Rhod 3-AM. Fluorescence microscopic examination revealed a significant increase in the fluorescence intensity of the cells under acidic conditions; this signal was suppressed by BAPTA-AM, the calcium

scavenger (Fig *5C*, *left*). To determine whether an increase in intracellular calcium is mediated through ASIC1, we performed the same experiment with LM-4142 ASIC1 KO and gRNA control cells. We detected an obvious increase in fluorescence intensity under acidic conditions in control cells, however, no such an increase was detected in ASIC1 KO cells (Fig *5C*, *right*), suggesting that ASIC1 can contribute to the calcium influx under acidic conditions.

ASIC1 is localized in mitochondria

Since mitochondrion is the major source of ROS, we asked whether ASIC1 is associated with mitochondria, leading to ROS production. We used cyclophilin F and mitochondrial calcium uniporter as mitochondrial markers (26). As expected, no ASIC1 was detected in ASIC1 KO cells (Fig *5D*). In control cells, ASIC1 was detected in mitochondria as well as other cellular components (supernatant) and whole cell extract. The association of ASIC1 with mitochondria was also examined by staining the cells with MitoTracker orange, the mitochondrial dye, and ASIC1 antibody. The ASIC1 signal was found only in control cells with distribution pattern identical to MitoTracker (Fig *5E*). Furthermore, an analysis of LM-4142 cells expressing ASIC1-GFP revealed co-localization of GFP with Mitotracker (Fig *S4A*), providing further evidence for mitochondrial localization of ASIC1. However, acidosis had no effect on mitochondrial content of ASIC1 (Fig *S4B*) or its distribution (Fig *S4C*).

ASIC1 is required for acidosis-induced AKT and ERK1/2 activation

Our previous report indicates that AKT is rapidly activated upon acidosis (5) and ERK1/2 are crucial signaling pathways that control diverse cellular processes including tumor cell invasion and metastasis. We determined whether inhibition of ASIC1 affects phosphorylation of AKT and ERK1/2. Consistent with previous observations, low pH medium induced AKT phosphorylation in a panel of breast cancer cell lines (Fig *S5A*). However, when cells were treated with ASIC1 inhibitors (amiloride or PcTx-1) before culture was exposed to low pH medium, AKT phosphorylation was suppressed in all cell lines tested. The low pH also induced phosphorylation of ERK1/2 that was suppressed by amiloride and PcTx-1 (Fig *S5B*). We also found that acidosis can induce ERK1/2 phosphorylation in MCF-7 and LM-4142 cells (Fig *S5C*). However, the kinetics of ERK1/2 phosphorylation was different in two cell lines; as early as after 5 minutes in MCF-7 cells and after 30 minutes in LM-4142 cells. Interestingly, an oscillation in ERK1/2 phosphorylation was observed in both cell lines, a pattern similar to what was observed for pAKT (5). These results suggest that ASIC1 activity is also required for phosphorylation of AKT and ERK1/2 in breast cancer cells.

Suppression of tumor growth by ASIC1 inhibitors (amiloride and PcTx-1)

To explore the therapeutic potential of targeting ASIC1, we first tested amiloride, a non-specific inhibitor for ASICs (27), to determine whether this molecule can inhibit tumor growth in a xenograft-mouse model. LM-4142 cells were xenograft-implanted into the mammary fat pads. Thirteen days later, mice were given water (vehicle) or amiloride (10 mg/kg body weight, *i.p.*, every other day) for 13 days (Fig *S6A*). Tumor growth had increased rapidly in the vehicle-treated group; however, in the amiloride group, tumor

growth was significantly suppressed from day 4 onwards (Fig *6A*). Moreover, the tumor weight was suppressed by 56% in the amiloride group as compared to vehicle group (Fig *6B, left*). An obvious difference in the tumor size was observed in the two groups (Fig *6B, right*). Amiloride had no effect on body weight (Fig *S6B*), indicating that mice are tolerant to this dose of amiloride.

We then tested the specific ASIC inhibitor PcTx-1 to further determine the role of ASIC1 inhibition in tumor growth. An intratumor injection of PcTx-1 reduced the tumor grwoth by 52% after 7 days in comparison to control group (Fig *6C, left*) with an obvious difference in the size of the tumors between the two groups of mice (Fig *6C, right*). These results suggest that ASIC1 may serve as a novel therapeutic target for breast cancer.

Clinical significance of ASIC1

To evaluate the clinical relevance of ASIC1, we analyzed ASIC1 mRNA expression in a cDNA array consisting of 7 normal and 41 breast cancer specimens from OriGene. Although the expression of ASIC1 was widely spread, we detected on average a 3.7-fold increase in the tumor specimens as compared to normal specimens (Fig *6D*). Furthermore, analysis of the stage I progression breast TMAs by immunohistochemistry also revealed an increase in ASIC1 expression in malignant specimens as compared to those in normal tissue. For example, strong ASIC1 expression was observed in 14.3% of malignant tissues while in normal tissues, no staining was observed (Fig *S7A*). However, although patients with upregulation of ASIC1 tended to have poor overall survival compared to those without upregulation of ASIC1, this association was not statistically significant (Fig *S7B*). In contrast, interrogation of the Cancer Genome Atlas (TCGA) Breast Invasive Carcinoma dataset at cBioPortal (http://www.cbioportal.org) (28, 29) indicated that 3.3% of 1098 samples carried alterations of ASIC1, including amplification, mutations and up-regulation (Fig S*7C*). More importantly, "percentage of overall survival" of the patients with ASIC1 alterations was significantly less than those without alterations in ASIC1 (Fig *6E*). For example, the "median survival months" for those cases with ASIC1 alterations was 77.56 while those without ASIC1 alterations was 114.06 (Fig *S7D*). Importantly, although only 3.3% of the samples carried ASIC1 alterations, when all five ASIC genes (ASIC1, ASIC2, ASIC3, ASIC4 and ASIC5) were pooled together, this number was increased to 18.6% (Fig. *S8A*). Of interest, there was little overlap among those ASIC genes. Alterations of five ASIC genes were significantly correlated to patient survival (Fig. *6F*) with median months survival of 83.8 for patients with ASIC alterations compared to 129.47 for patients without ASIC alterations (Fig. *S8B*). Together, these results suggest that ASICs may serve as a marker to predict the overall survival.

DISCUSSION

The extracellular pH (pHe) of solid tumors, such as breast tumors, is often acidic primarily due to high glycolysis and poor perfusion within tumors; pHe values could reach 6.2~6.8 (30). Acidosis in the tumor microenvironment has been shown to produce multiple effects on tumorigenesis. For instance, acidosis has been implicated in invasive and metastatic progression of breast cancer. However, little is known how tumor cells sense the acidic

signal in tumor microenvironment and then activate the acidosis-mediated signaling, leading to aggressiveness of tumor cells. The present study demonstrates that neuron specific ASIC1 can also be functionally expressed in breast cancer cells. More importantly, this channel is required for acidosis-induced ROS generation and tumor cell invasion. In animal models, ASIC1 is required for primary tumor growth and metastasis of breast cancer. Together, these findings support a critical role for ASIC1 in breast cancer pathogenesis.

Acidity is harmful to normal cell growth and proliferation. However, during a long time of co-evolution with the host, tumor cells have adapted well to acidic tumor microenvironment. For example, tumor cells can employ various mechanisms to remove intracellular acids in order to maintain physiological pHi. These include Na-driven proton extrusion, V-type ATPases, Na^+/H^+ exchangers (NHEs) and those facilitated by carbonic anhydrases (8). As a result, pHe becomes more acidic. A key question is how tumor cells sense the acidic microenvironment and then transduce into the cell to impact gene expression. Identification of ASIC1 function in breast cancer in this study provides a plausible explanation as to why acidic conditions are beneficial to tumor cells for their advances.

In support of this notion, ASIC1 is highly expressed in malignant tissues, which may in part attribute to the capability of ASIC1 to promote cell invasion and metastasis. That "overall survival" of patients with tumors exhibiting genetic alterations in ASIC1 expression was significantly reduced further substantiates the clinical relevance of this ion channel for breast cancer. Although TCGA dataset does not contain tumor subtype information, it lists clinical features such as ER, PR and HER2. We found that genetic alterations of ASIC1 are not associated with any of these features. Furthermore, ASIC1 siRNAs as well as ASIC1 inhibitors (amiloride and PcTx-1) are capable of suppressing tumor growth and tumor weight in a xenograft mouse model, suggesting that ASIC1 may serve as a potential target for cancer therapy. Given that extracellular acidosis is a common feature for solid tumors, these findings may have a broad impact. Thus, it is conceivable that ASIC1-mediated tumor cell invasion and metastasis can also occur in other types of solid tumors.

Several lines of evidence support that ASIC1-mediated ROS generation and activation of downstream targets such as NF-κB in response to acidosis may serve as a major contributor to breast tumorigenesis (Fig *S9*). *First*, ROS scavengers has been shown to suppress acidosis induced invasion activity of breast cancer cells (5). ASIC1 knockout abrogates acidosis-induced ROS production. *Second*, re-expression of ASIC1 in the KO cells restores ROS production. *Third*, ASIC1 inhibitors suppress acidosis-induced ROS production. *Fourth,* regulation of ROS production by ASIC1 is specific to acidosis because ASIC1 KO has no effect on the H_2O_2-induced ROS production. *Finally*, it is known that oxidative stress activates ERK1/2 and AKT (31) and acidosis can activate AKT and NF-κB (5). All of these effects can be mediated through ASIC1 because ASIC1 inhibitors or ASIC siRNAs are able to suppress acidosis-induced activation of ERK1/2, AKT and NF-κB. The observations that acidosis induced activation of ERK1/2 and AKT, and ROS production was suppressed by ASIC1 inhibitors in a panel of breast cancer cell lines signifies the relevance of ASIC1 for many breast cancers. Furthermore, even minimal ASIC1 may be sufficient to affect acidosis mediated signaling pathways. Previously, we have shown that ROS generated under acidic conditions can inactivate PTEN thereby activating AKT (5). We now show that ASIC1 is

required for acidosis induced ROS generation. This suggests that ROS is a central molecule by which ASIC1 can regulate AKT activation in acidic microenvironment.

It is known that acidosis can activate ASIC channels and that this activation leads to a rise in intracellular Ca^{2+} ($[Ca^{2+}]_i$) in neurons (11). Part of this rise is due to direct entry of Ca^{2+} along with Na^+ through ASIC1 containing channels (23). This alteration of $[Ca^{2+}]_i$ triggers a cascade of events including membrane depolarization, activation of voltage-gated Ca^{2+} channels (VGCCs) and initiation of the main Ca^{2+} influx (32). Furthermore, elevation in $[Ca^{2+}]_i$ leads to its uptake by mitochondria, activation of electron transport chain, and subsequent generation of ROS (33). The cytoplasmic $[Ca^{2+}]_i$ can also activate ROS through NADPH oxidase in neutrophils (34) and neurons (35).

Calcium has been implicated as a crucial mediator of cancer cell migration and invasion (36). We show that ROS production was significantly suppressed by calcium chelators, suggesting that ASIC1-regulated calcium content is crucial for ROS production under acidic conditions. However, the relative permeability of ASIC1 for Ca^{2+} is relatively low (32). It is likely that ASIC1 acts like an initiator and the entry of Ca^{2+} through ASIC1 leads to a rise in $[Ca^{2+}]_i$, membrane depolarization, activation of voltage-gated Ca^{2+} channels (VGCCs) and the initiation of the main Ca^{2+} influx (32). There are two possibilities by which $[Ca^{2+}]_i$ can induce ROS production under acidic conditions: i) activation of mitochondrial electron transport chain (34, 35), and ii) modulation of calcium/calmodulin dependent NOX-5 activities (37, 38).

Although mitochondria is known as one of the Ca^{2+} storage organelles (39), it is not clear whether ASIC1 is involved in the regulation of mitochondrial Ca^{2+} homeostasis. We demonstrate that ASIC1 is localized in mitochondria, which may contribute to mitochondrial Ca^{2+} influx mechanisms like mitochondrial calcium uniporter. However, mitochondrial contents of ASIC1 and calcium (unpublished data) was unchanged by low pH conditions. Calcium signaling takes a variety of forms in space and time and is based on Ca^{2+} circulation among four primary compartments: extracellular space, cytoplasm, endoplasmic reticulum and mitochondria (40). The calcium entry into the mitochondria through ASIC1 can be counteracted by exchangers such as the Na^+/Ca^{2+} exchanger to re-circulate Ca^{2+} back into the cytosol (41). While transient elevations in mitochondrial calcium are important for modulation of cell signaling pathways such as activation of electron transport chain (42), prolonged accumulation is a source for cytochrome c release and induction of apoptosis (43). Cancer cells might have developed Ca^{2+} exchangers as a mechanism to reduce mitochondrial Ca^{2+} accumulation and to evade apoptosis under acidic conditions. Regarding the second possibility, NOX-5 has a unique amino terminus that encodes four calcium binding EF-hands (44). These EF-hands serve as a sensor to the elevation in intracellular calcium that triggers intramolecular conformational changes in the enzyme (45). This permits the interaction of the N terminus of NOX-5 with its C-terminal domain, which then facilitates electron transport and ROS production (46). Our unpublished observations indicate that breast cancer cells express NOX5, which may serve as a potential regulator for ASIC1-mediated ROS generation. Therefore, a better understanding of ASIC1-mediated ROS generation, and activation of the associated signaling pathways will provide new

insight into cancer biology in the context of the interaction between tumor cells and the acidic tumor microenvironment, leading to invasion and metastasis.

MATERIALS AND METHODS

Cell culture

Details of cell culture were described in supplementary materials. The pH of the culture medium was adjusted to 6.6 with 20 mM 2-(N-morpholino)ethane-sulphonic acid and 20 mM Tris (hydroxymethyl) aminomethane. MCF-7, T47D and MDA-MB-231 cells were authenticated by DDC Medical (http://www.ddcmedical.com) using the short tandem repeat profiling method.

Invasion assay

To examine cell invasion activity *in vitro*, we used BD BioCoat tumor invasion system and followed a method described previously from the laboratory (5). In brief, cells were cultured at pH 7.4 or pH 6.6 for 48 hours and then assessed *in vitro* in regular medium using Matrigel invasion chambers. Since regular culture medium often becomes acidic after cells are grown for a period of time, we replaced with fresh medium after every 10-12 hours.

Mitochondria labeling and subcellular localization of ASIC1

To examine the subcellular localization of ASIC1, we labeled mitochondria with MitoTracker® Orange following the manufacturer's instructions. The procedure for staining the cells with primary and secondary antibodies and for imaging has been described before (5).

Immunohistochemistry

We used the Stage I Breast Progression TMA from NCI Cancer Diagnosis Program (CDP) for detection of ASIC1 by immunohistochemistry (IHC) following a method described before (51).

Transfection

Cells were transfected with siRNAs using RNAfectin reagent or plasmid DNA using DNAfectin (47).

Measurement of intracellular ROS

We used membrane-permeable DCFH-DA dye for GFP negative cells and CellROX® Deep Red Reagent for GFP positive cells. Cells were cultured under normal or low pH medium in the presence of dye and the intracellular ROS generation was measured by flow cytometry (48).

Western blot analysis

The protein extract from mitochondrial and whole cell extracts were prepared, and Western blot analysis was carried out as described earlier (5).

Preparation of mitochondrial extracts

Mitochondria from cultured cells were isolated using Abcam's mitochondria isolation kit, essentially following the manufacturer's instructions.

Electrophysiological recordings

We used whole-cell patch-clamp mode to record acid-induced ASIC currents at room temperature with an Axopatch 200B amplifier (Axon Instruments, FosterCity, CA). The currents were acquired using p-CLAMP software (version 10; Axon Instruments) at a rate of 10 kHz and data analysis was performed using Clamp fit software (version 10.0; Axon Instruments) (23, 49).

Constructs

The high fidelity Phusion enzyme from NEB (Ipswich, MA) was used to amplify DNA fragments by PCR for cloning purpose. To clone Myc-ASIC1, we first amplified the ASIC1 coding region using primers ASIC1-Myc-R1-5.1 and ASIC1-Not1-3.1, and then cloned into pCDH-Myc by Cold Fusion kit (System Bioscience) as described previously (50). To make ASIC1-GFP fusion, we amplified GFP using primers PCDH-R1-5.1 and GFP-ASIC1-3.1, and the ASIC1 coding region using primers GFP-ASIC1-5.1 and ASIC1-Sal1-3.1, respectively. These two overlapping fragments were subsequently cloned into pCDH by Cold Fusion kit. Dual gRNA targeting ASIC1 exon 2 and 3, and ASIC1 donor were constructed using same method as described previously (21). For ASIC1 donor vector, we used primer sets ASIC1-left-BamH1-5.1 and ASIC1-left-BamH1-3.1 (left arm), and ASIC1-right-R1-5.1 and ASIC1-right-R1-5.1 (right arm). These two fragments were sequentially cloned into donor vector at BamH I and EcoR I sites. All amplified fragments were verified by DNA sequencing.

Intracellular calcium measurement

The intracellular calcium was measured using a Rhod-3 calcium imaging kit. LM-4142 cells were loaded with Rhod 3-AM for 30 min in the presence of $1\times$ PowerLoad concentrate and 2.5 mM probenecid and then examined under the fluorescence microscope.

Experimental protocol for animal work

The animal studies were conducted in accordance with NIH animal use guidelines and the experimental protocol was approved by the UMMC's Animal Care and Use Committee. LM-4142 cells transfected with ASIC1 siRNA were harvested at the exponential stage and then resuspended in a 50%:50% solution of PBS and matrigel, and injected into the mammary fat pad (51). Seven days after tumor implantation, primary tumor outgrowth was monitored every other day by taking measurements of the tumor length (L) and width (W) and tumor volume was calculated using the formula $1/2 \times L \times W^2$ (52). At the end of the experiment, tumor was excised and weight was taken. To test effect of amiloride on tumor growth, mice implanted with LM-4142 cells were stratified by initial weight and then block randomization was applied to each strata to randomize the mice to the following treatment groups (6 mice/group): (i) untreated control (100 μL water, i.p., every other day for 13 days), and (ii) amiloride (10 mg/kg body weight, i.p., every other day for 13 days). To test the effect of

psalmotoxin 1, tumor bearing mice were intratumorally injected with psalmotoxin 1 (25 ng/kg body weight) every other day for 7 days and tumor volume was measured as indicated above. For metastasis studies, LM-4142 cells were injected into nude mice through tail vein (1×10^6 cells/ mouse). Six weeks after injection, mice were sacrificed, lungs were harvested, fixed in Bouin's solution and images were captured.

Statistical methods

Although the researchers conducting the experiments were not blinded to the group allocation, statistician was blinded from group allocation when performing statistical analyzes. The continuous outcomes were summarized as mean and standard error of the mean (SEM). The normality of data was checked by the stem and leaf plot and the data were approximately normal. The two-sample t test was used to compare the mean of continuous outcome between two experimental conditions. The Satterthwaite t test was used when unequal variances were confirmed by Levene's test. The Bonferroni correction was applied in the experiments involving comparisons at multiple time points or among more than two experimental conditions. The Kaplan-Meier method was used to estimate the survival probability in subgroups determined by expression level or alteration status of ASIC1. Comparison of the survival between subgroups was evaluated by the log-rank test. All P values were two-sided and P values less than 0.05 were considered as significant. Statistical analysis was performed using the software SAS (version 9.3, the SAS institute). We used cBioPortal dataset and survival analysis output to evaluate the association of ASIC1 genetic alterations with survival of breast cancer patients (28, 29).

The sample size calculation was performed for two animal experiments in which the mean tumor volume would be compared between two experimental conditions. We conservatively estimated the effect size to be 2 standard deviation. At the 5% level, the size of 6 mice per group was required to yield the power of 90% for detecting the effect size of 2 using a two-sided t test. The actual mice numbers used in these two experiments were 6 or 8 mice per group as indicated in figure legends. Therefore, the size requirement was met and we had sufficient power for tumor volume comparison.

Supplementary Material

Refer to Web version on PubMed Central for supplementary material.

ACKNOWLEDGEMENTS

REFERENCES

1. Gatenby RA, Gillies RJ. Why do cancers have high aerobic glycolysis? Nature reviews Cancer. 2004; 4(11):891–9. [PubMed: 15516961]

2. Abbey CK, Borowsky AD, McGoldrick ET, Gregg JP, Maglione JE, Cardiff RD, et al. In vivo positron-emission tomography imaging of progression and transformation in a mouse model of

mammary neoplasia. Proceedings of the National Academy of Sciences of the United States of America. 2004; 101(31):11438–43. [PubMed: 15277673]

3. Estrella V, Chen T, Lloyd M, Wojtkowiak J, Cornnell HH, Ibrahim-Hashim A, et al. Acidity generated by the tumor microenvironment drives local invasion. Cancer research. 2013; 73(5):1524–35. [PubMed: 23288510]

4. Robey IF, Baggett BK, Kirkpatrick ND, Roe DJ, Dosescu J, Sloane BF, et al. Bicarbonate increases tumor pH and inhibits spontaneous metastases. Cancer research. 2009; 69(6):2260–8. [PubMed: 19276390]

5. Gupta SC, Singh R, Pochampally R, Watabe K, Mo YY. Acidosis promotes invasiveness of breast cancer cells through ROS-AKT-NF-kappaB pathway. Oncotarget. 2014

6. Xu L, Fidler IJ. Acidic pH-induced elevation in interleukin 8 expression by human ovarian carcinoma cells. Cancer research. 2000; 60(16):4610–6. [PubMed: 10969814]

7. Peppicelli S, Bianchini F, Contena C, Tombaccini D, Calorini L. Acidic pH via NF-kappaB favours VEGF-C expression in human melanoma cells. Clinical & experimental metastasis. 2013; 30(8): 957–67. [PubMed: 23784694]

8. Damaghi M, Wojtkowiak JW, Gillies RJ. pH sensing and regulation in cancer. Frontiers in physiology. 2013; 4:370. [PubMed: 24381558]

9. Wemmie JA, Askwith CC, Lamani E, Cassell MD, Freeman JH Jr. Welsh MJ. Acid-sensing ion channel 1 is localized in brain regions with high synaptic density and contributes to fear conditioning. The Journal of neuroscience : the official journal of the Society for Neuroscience. 2003; 23(13):5496–502. [PubMed: 12843249]

10. Schaefer L, Sakai H, Mattei M, Lazdunski M, Lingueglia E. Molecular cloning, functional expression and chromosomal localization of an amiloride-sensitive Na(+) channel from human small intestine. FEBS letters. 2000; 471(2-3):205–10. [PubMed: 10767424]

11. Waldmann R, Champigny G, Bassilana F, Heurteaux C, Lazdunski M. A proton-gated cation channel involved in acid-sensing. Nature. 1997; 386(6621):173–7. [PubMed: 9062189]

12. Chu XP, Xiong ZG. Physiological and pathological functions of acid-sensing ion channels in the central nervous system. Current drug targets. 2012; 13(2):263–71. [PubMed: 22204324]

13. Berdiev BK, Xia J, McLean LA, Markert JM, Gillespie GY, Mapstone TB, et al. Acid-sensing ion channels in malignant gliomas. The Journal of biological chemistry. 2003; 278(17):15023–34. [PubMed: 12584187]

14. Bubien JK, Keeton DA, Fuller CM, Gillespie GY, Reddy AT, Mapstone TB, et al. Malignant human gliomas express an amiloride-sensitive Na+ conductance. The American journal of physiology. 1999; 276(6 Pt 1):C1405–10. [PubMed: 10362604]

15. Wemmie JA, Taugher RJ, Kreple CJ. Acid-sensing ion channels in pain and disease. Nature reviews Neuroscience. 2013; 14(7):461–71. [PubMed: 23783197]

16. Wemmie JA, Chen J, Askwith CC, Hruska-Hageman AM, Price MP, Nolan BC, et al. The acid-activated ion channel ASIC contributes to synaptic plasticity, learning, and memory. Neuron. 2002; 34(3):463–77. [PubMed: 11988176]

17. Bianchi L, Driscoll M. Protons at the gate: DEG/ENaC ion channels help us feel and remember. Neuron. 2002; 34(3):337–40. [PubMed: 11988165]

18. Ugawa S, Ueda T, Ishida Y, Nishigaki M, Shibata Y, Shimada S. Amiloride-blockable acid-sensing ion channels are leading acid sensors expressed in human nociceptors. The Journal of clinical investigation. 2002; 110(8):1185–90. [PubMed: 12393854]

19. Chen X, Kalbacher H, Grunder S. The tarantula toxin psalmotoxin 1 inhibits acid-sensing ion channel (ASIC) 1a by increasing its apparent H+ affinity. The Journal of general physiology. 2005; 126(1):71–9. [PubMed: 15955877]

20. Jinek M, Chylinski K, Fonfara I, Hauer M, Doudna JA, Charpentier E. A programmable dual-RNA-guided DNA endonuclease in adaptive bacterial immunity. Science. 2012; 337(6096):816–21. [PubMed: 22745249]

21. Ho TT, Zhou N, Huang J, Koirala P, Xu M, Fung R, et al. Targeting non-coding RNAs with the CRISPR/Cas9 system in human cell lines. Nucleic acids research. 2015; 43(3):e17. [PubMed: 25414344]

22. Minn AJ, Gupta GP, Siegel PM, Bos PD, Shu W, Giri DD, et al. Genes that mediate breast cancer metastasis to lung. Nature. 2005; 436(7050):518–24. [PubMed: 16049480]

23. Xiong ZG, Zhu XM, Chu XP, Minami M, Hey J, Wei WL, et al. Neuroprotection in ischemia: blocking calcium-permeable acid-sensing ion channels. Cell. 2004; 118(6):687–98. [PubMed: 15369669]

24. Brookes PS, Yoon Y, Robotham JL, Anders MW, Sheu SS. Calcium, ATP, and ROS: a mitochondrial love-hate triangle. American journal of physiology Cell physiology. 2004; 287(4):C817–33. [PubMed: 15355853]

25. Viola HM, Arthur PG, Hool LC. Transient exposure to hydrogen peroxide causes an increase in mitochondria-derived superoxide as a result of sustained alteration in L-type Ca2+ channel function in the absence of apoptosis in ventricular myocytes. Circulation research. 2007; 100(7): 1036–44. [PubMed: 17347474]

26. Giorgio V, Soriano ME, Basso E, Bisetto E, Lippe G, Forte MA, et al. Cyclophilin D in mitochondrial pathophysiology. Biochimica et biophysica acta. 2010; 1797(6-7):1113–8. [PubMed: 20026006]

27. Benarroch EE. Acid-sensing cation channels: structure, function, and pathophysiologic implications. Neurology. 2014; 82(7):628–35. [PubMed: 24443451]

28. Gao J, Aksoy BA, Dogrusoz U, Dresdner G, Gross B, Sumer SO, et al. Integrative analysis of complex cancer genomics and clinical profiles using the cBioPortal. Science signaling. 2013; 6(269):pl1. [PubMed: 23550210]

29. Cerami E, Gao J, Dogrusoz U, Gross BE, Sumer SO, Aksoy BA, et al. The cBio cancer genomics portal: an open platform for exploring multidimensional cancer genomics data. Cancer discovery. 2012; 2(5):401–4. [PubMed: 22588877]

30. Hashim AI, Zhang X, Wojtkowiak JW, Martinez GV, Gillies RJ. Imaging pH and metastasis. NMR in biomedicine. 2011; 24(6):582–91. [PubMed: 21387439]

31. McCubrey JA, Lahair MM, Franklin RA. Reactive oxygen species-induced activation of the MAP kinase signaling pathways. Antioxidants & redox signaling. 2006; 8(9-10):1775–89. [PubMed: 16987031]

32. Zha XM. Acid-sensing ion channels: trafficking and synaptic function. Molecular brain. 2013; 6:1. [PubMed: 23281934]

33. Feissner RF, Skalska J, Gaum WE, Sheu SS. Crosstalk signaling between mitochondrial Ca2+ and ROS. Front Biosci (Landmark Ed). 2009; 14:1197–218. [PubMed: 19273125]

34. Granfeldt D, Samuelsson M, Karlsson A. Capacitative Ca2+ influx and activation of the neutrophil respiratory burst. Different regulation of plasma membrane- and granule-localized NADPH-oxidase. Journal of leukocyte biology. 2002; 71(4):611–7. [PubMed: 11927647]

35. Wang G, Anrather J, Glass MJ, Tarsitano MJ, Zhou P, Frys KA, et al. Nox2, Ca2+, and protein kinase C play a role in angiotensin II-induced free radical production in nucleus tractus solitarius. Hypertension. 2006; 48(3):482–9. [PubMed: 16894058]

36. Prevarskaya N, Skryma R, Shuba Y. Calcium in tumour metastasis: new roles for known actors. Nature reviews Cancer. 2011; 11(8):609–18. [PubMed: 21779011]

37. El Jamali A, Valente AJ, Lechleiter JD, Gamez MJ, Pearson DW, Nauseef WM, et al. Novel redox-dependent regulation of NOX5 by the tyrosine kinase c-Abl. Free radical biology & medicine. 2008; 44(5):868–81. [PubMed: 18160052]

38. Pandey D, Gratton JP, Rafikov R, Black SM, Fulton DJ. Calcium/calmodulin-dependent kinase II mediates the phosphorylation and activation of NADPH oxidase 5. Molecular pharmacology. 2011; 80(3):407–15. [PubMed: 21642394]

39. Rizzuto R, Pozzan T. Microdomains of intracellular Ca2+: molecular determinants and functional consequences. Physiological reviews. 2006; 86(1):369–408. [PubMed: 16371601]

40. Berridge MJ, Bootman MD, Lipp P. Calcium--a life and death signal. Nature. 1998; 395(6703): 645–8. [PubMed: 9790183]

41. Drago I, Pizzo P, Pozzan T. After half a century mitochondrial calcium in- and efflux machineries reveal themselves. The EMBO journal. 2011; 30(20):4119–25. [PubMed: 21934651]

42. Berridge MJ, Lipp P, Bootman MD. The versatility and universality of calcium signalling. Nature reviews Molecular cell biology. 2000; 1(1):11–21. [PubMed: 11413485]

43. Pinton P, Giorgi C, Siviero R, Zecchini E, Rizzuto R. Calcium and apoptosis: ER-mitochondria Ca2+ transfer in the control of apoptosis. Oncogene. 2008; 27(50):6407–18. [PubMed: 18955969]

44. Banfi B, Molnar G, Maturana A, Steger K, Hegedus B, Demaurex N, et al. A Ca(2+)-activated NADPH oxidase in testis, spleen, and lymph nodes. The Journal of biological chemistry. 2001; 276(40):37594–601. [PubMed: 11483596]

45. Jagnandan D, Church JE, Banfi B, Stuehr DJ, Marrero MB, Fulton DJ. Novel mechanism of activation of NADPH oxidase 5. calcium sensitization via phosphorylation. The Journal of biological chemistry. 2007; 282(9):6494–507. [PubMed: 17164239]

46. Banfi B, Tirone F, Durussel I, Knisz J, Moskwa P, Molnar GZ, et al. Mechanism of Ca2+ activation of the NADPH oxidase 5 (NOX5). The Journal of biological chemistry. 2004; 279(18):18583–91. [PubMed: 14982937]

47. Zhang A, Zhou N, Huang J, Liu Q, Fukuda K, Ma D, et al. The human long non-coding RNA-RoR is a p53 repressor in response to DNA damage. Cell research. 2013; 23(3):340–50. [PubMed: 23208419]

48. Gupta SC, Francis SK, Nair MS, Mo YY, Aggarwal BB. Azadirone, a limonoid tetranortriterpene, induces death receptors and sensitizes human cancer cells to tumor necrosis factor-related apoptosis-inducing ligand (TRAIL) through a p53 protein-independent mechanism: evidence for the role of the ROS-ERK-CHOP-death receptor pathway. The Journal of biological chemistry. 2013; 288(45):32343–56. [PubMed: 24078627]

49. Ye JH, Gao J, Wu YN, Hu YJ, Zhang CP, Xu TL. Identification of acid-sensing ion channels in adenoid cystic carcinomas. Biochemical and biophysical research communications. 2007; 355(4): 986–92. [PubMed: 17324378]

50. Sachdeva M, Mo YY. MicroRNA-145 suppresses cell invasion and metastasis by directly targeting mucin 1. Cancer research. 2010; 70(1):378–87. [PubMed: 19996288]

51. Huang J, Zhou N, Watabe K, Lu Z, Wu F, Xu M, et al. Long non-coding RNA UCA1 promotes breast tumor growth by suppression of p27 (Kip1). Cell death & disease. 2014; 5:e1008. [PubMed: 24457952]

52. Tomayko MM, Reynolds CP. Determination of subcutaneous tumor size in athymic (nude) mice. Cancer chemotherapy and pharmacology. 1989; 24(3):148–54. [PubMed: 2544306]
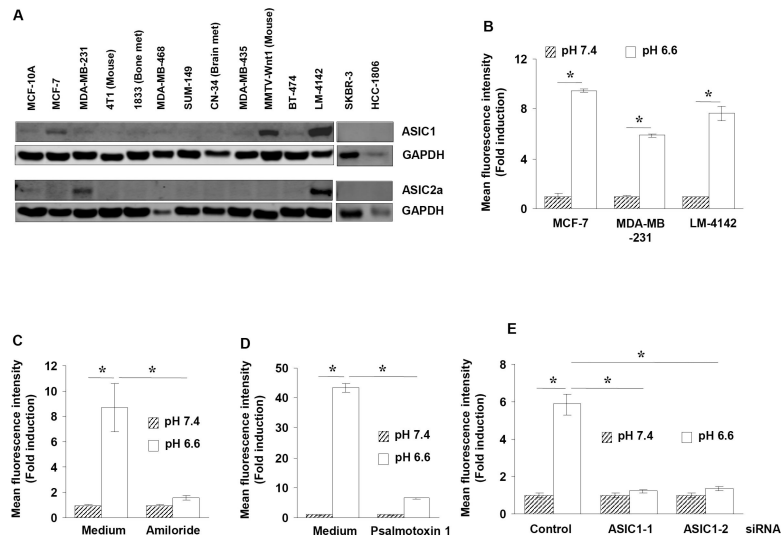
Figure 1. Acidosis-induced ROS production is mediated through ASIC1 in breast cancer cells

(*A*) The whole cell extract from indicated cells were examined for the expression of ASIC isoforms by Western blotting. (*B*) Cells were cultured under normal or acidic medium for 1 h and intracellular ROS level was measured using the ROS stain, DCFH-DA. Values indicate mean ± SEM (n = 3). (*C, D*) MCF-7 cells were cultured at pH 7.4 or pH 6.6 without and with ASIC1 inhibitors (100 μM amiloride or 100 nM psalmotoxin 1) and analyzed for intracellular ROS levels. Values indicate mean ± SEM (n = 6 for *C*, and 3 for *D*). (E) The siRNA transfected MCF-7 cells were cultured under normal or acidic medium for 1h and assessed for intracellular ROS levels. Values indicate mean ± SEM (n = 6). *, $P < 0.05$.
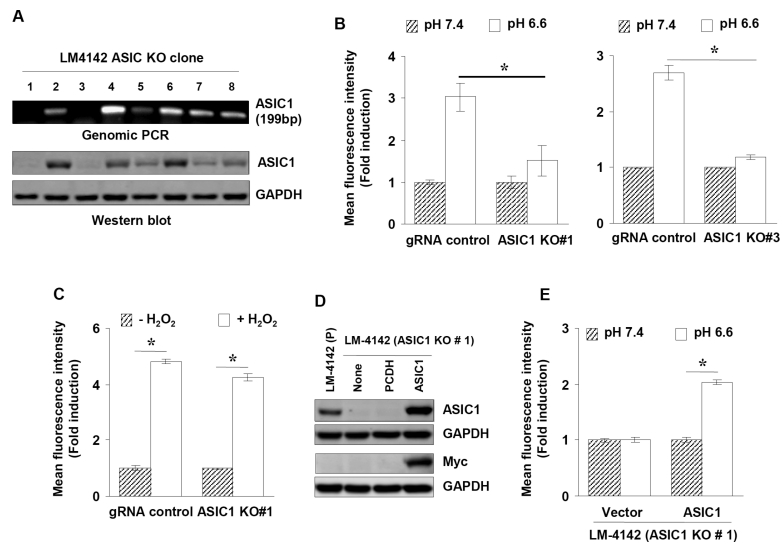
Figure 2. ASIC1 knock-out impairs the intracellular ROS generation in breast cancer cells under acidic conditions

(*A*) Detection of LM-4142 ASIC1 KO cell lines by western blotting and PCR. (*B*) LM-4142 cells (gRNA control and ASIC1 KO) were cultured at pH 7.4 or pH 6.6 for 1 h and analyzed for intracellular ROS levels. Values indicate mean ± SEM (n = 11 for KO # 1, and 6 for KO # 3). (*C*) ASIC1 knockout and gRNA control cells were exposed to H_2O_2 (10 mM) for 1 h in normal medium before analysis for intracellular ROS generation. Values indicate mean ± SEM (n = 3). (*D*) The expression vector carrying Myc-tagged ASIC1 or vector alone was introduced into LM-4142 ASIC1 KO#1 cells, whole cell extract was used to analyze ASIC1 and Myc tag; (*E*) cells were cultured at pH 7.4 or pH 6.6 for 1 hour and analyzed for intracellular ROS levels. Values indicate mean ± SEM (n = 4). *, $P < 0.05$.
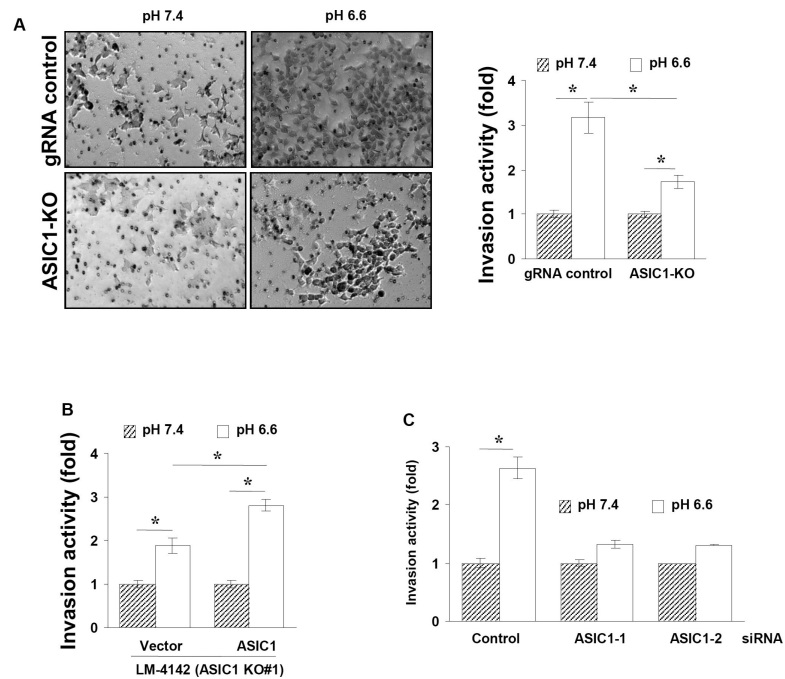
Figure 3. The invasion activity of breast cancer cells under acidic conditions is mediated through ASIC1

(*A*) LM-4142 cells (gRNA control and ASIC1 KO) were cultured under normal or low pH medium for 24 hours and assessed *in vitro* for invasion activity. Values indicate mean ± SEM (n = 4). (*B*) ASIC1 overexpressing cells were cultured under normal or acidic medium for 24 hours and then used to assess invasion activity. Values indicate mean ± SEM (n = 4). (*C*) The siRNA transfected cells were cultured under normal or acidic medium for 24 hours and assessed *in vitro* for invasion activity. Values indicate mean ± SEM (n = 3). *, *P*< 0.05.
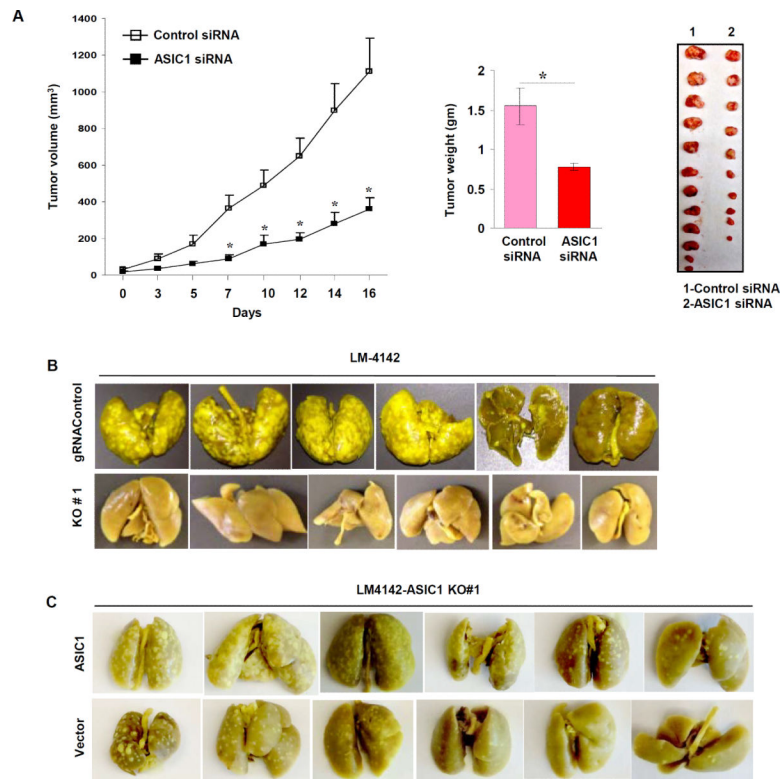
Figure 4. ASIC1 is required for tumor growth and lung metastasis in nude mice

(*A, left*) Tumor volume measured on various days; data represent mean ± SEM of tumor volume of 8 mice in each group. (*A, middle*) tumor weight at the end of the experiment. *, $P < 0.05$ (control siRNA vs ASIC1 siRNA). (*A, right*) Actual tumors from two groups at the end of the experiment. (*B*) Cells (gRNA control or ASIC1 KO) were injected into the female nude mice through tail vein. Six weeks after injection, mice were sacrificed, lungs were harvested and fixed in Bouin's solution and images were captured. (*C*) ASIC1 KO cells (with ASIC1 or vector alone) were injected into the nude mice and processed as in (*B*).
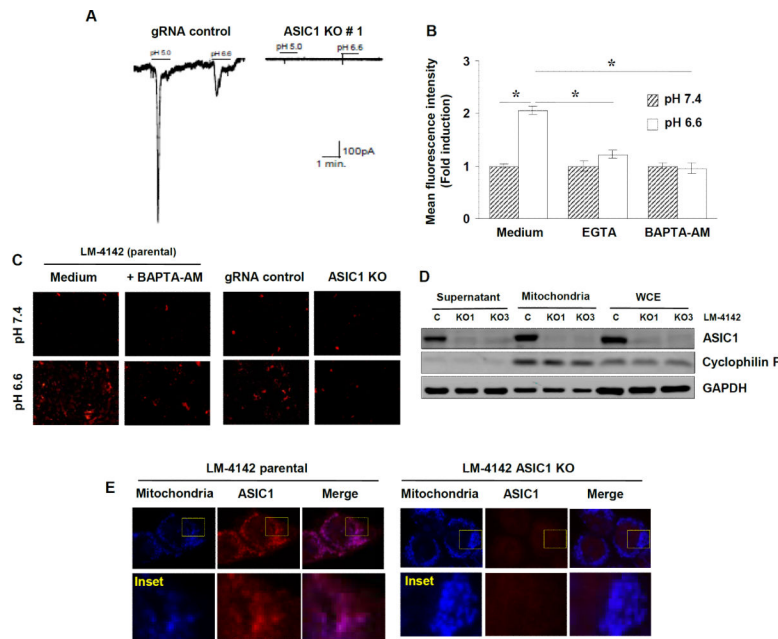
Figure 5. ASIC1 is functional in LM-4142 cells

(*A*) Low pH induces ASIC currents in LM-4142 cells; KO cells does not respond to acidic stimuli. (*B*) LM-4142 cells were pretreated with calcium scavengers (10 μM EGTA or 10 μM BAPTA-AM) for 30 min, cultured under normal or low pH conditions for 1 h and analyzed for intracellular ROS levels. Values indicate mean ± SEM (n= 4). *, *P*< 0.05. (*C*) LM-4142 cells (parental, gRNA control or ASIC1 KO) were loaded with calcium loading dye, Rhod-3AM without or with 10 μM BAPTA-AM (calcium scavenger) and examined under the fluorescence microscope. (*D*) The mitochondrial preparations from LM-4142 cells (gRNA control and ASIC1 KO) along with post-spin supernatant and whole cell extract were examined for ASIC1 and organelle markers (cyclophilin F for mitochondria, GAPDH for cytosol). (*E*) Fluorescence images of LM-4142 cells stained with mitotracker orange (blue) and ASIC1 (red). Insets are enlarged images of selected fields.
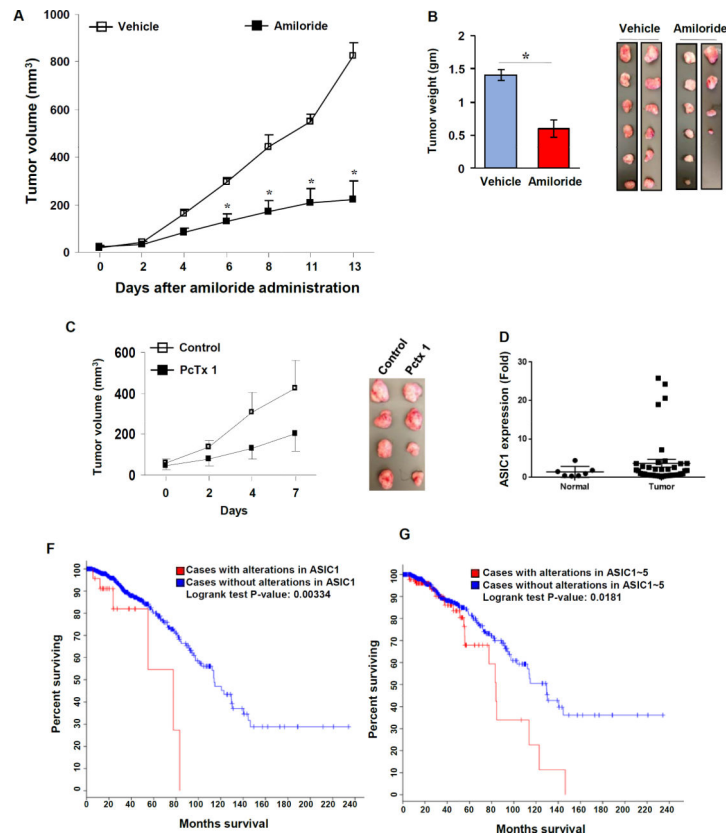
Figure 6. ASIC1 can serve as a therapeutic target and predict outcomes in breast cancer
(*A*) Tumor growth after administration of amiloride, ASIC inhibitor. Values represent mean ± SEM of tumor volume of 6 mice in each group. (*B*) Tumor weight at the end of the experiment (*left*). *, *P*< 0.05 (vehicle vs amiloride). Actual tumors from two groups at the end of the experiment (*right*). (*C*) Two weeks after tumor implantation, when tumor reached the volume of less than 100 mm³, mice were intratumorally injected with PcTx-1 (25 ng/kg body weight) every other day for 7 days. (*Left*) tumor volume on various days. (*Right*) Actual tumors from two groups at the end of the experiment. (*D*) ASIC1 mRNA expression in breast cancer cDNA array. (*E*) Kaplan-Meier plot comparing overall survival between cases without or with ASIC1 alterations. Onco Query Language (OQL) setting was "ASIC1: MUT AMP EXP>2.5" (*F*) Overall survival for five genes (ASIC1~5). OQL setting was "ASIC1: MUT AMP EXP>2.5; ASIC2: MUT AMP EXP>2.5; ASIC3: MUT AMP EXP>2.5; ASIC4: MUT AMP EXP>2.5; ASIC5: MUT AMP EXP>2.5".